

Search for $T = \frac{3}{2}$ States in ${}^5\text{Li}$, ${}^5\text{He}$, and ${}^5\text{H}^\dagger$

ROBERT L. MCGRATH, JOSEPH CERNY, AND S. W. COSPER*

Department of Chemistry and Lawrence Radiation Laboratory, University of California, Berkeley, California

(Received 1 September 1967)

Three experiments to search for $T = \frac{3}{2}$ mass-5 analog states have been performed. Both triton energy spectra from the ${}^7\text{Li}(p,t){}^5\text{Li}$ reaction and particle-particle coincidence data on the ${}^7\text{Li}(p,t){}^5\text{Li}$ and ${}^7\text{Li}(p,{}^3\text{He}){}^5\text{He}$ reactions failed to reveal well-defined ${}^5\text{Li}$ or ${}^5\text{He}$ states having expected $T = \frac{3}{2}$ properties. Tentative evidence is found from these measurements for broad $T = \frac{3}{2}$ states at 22-, 25-, and 34-MeV excitation energy. ${}^8\text{B}$ energy spectra from the ${}^9\text{Be}(\alpha,{}^8\text{B}){}^5\text{H}$ reaction also exhibited no peaks which might be associated with sharp states of ${}^5\text{H}$. These results are qualitatively in agreement with several theoretical predictions that ${}^5\text{H}$ is unbound to particle emission by at least several MeV.

I. INTRODUCTION

THE problem of the existence of the ${}^5\text{H}$ isotope has been the subject of numerous investigations.¹ A comprehensive review of the literature has been given by Baž *et al.*² Most experimenters have attempted to observe β^- activity from the ${}^5\text{H}$ ground state, with almost unanimously negative results. Consequently, while the consensus seems to be that ${}^5\text{H}$ is unbound to particle emission, little information has been available concerning the properties of possible virtual states of ${}^5\text{H}$. Data from one of the few experiments capable of observing such states, in which the ${}^7\text{Li}(\pi^-,d){}^5\text{H}$ reaction was observed, exhibited no deuteron peaks corresponding to well-defined states of ${}^5\text{H}$, but were labeled "inconclusive" by the authors³ because of a large continuum background.

Alternatively, studies on the $T = \frac{3}{2}$ analog states of ${}^5\text{He}$ and ${}^5\text{Li}$ can provide useful information on the mass and width of ${}^5\text{H}$ states. If ${}^5\text{H}$ is particle stable, then the lowest $T = \frac{3}{2}$ state of ${}^5\text{He}$ should occur below 19.5 MeV. However, three recent theoretical calculations indicate that the lowest $T = \frac{3}{2}$ state of ${}^5\text{He}$ lies considerably higher, at about 23 MeV,⁴ 24 MeV,⁵ or 26 MeV.⁶ Noting Fig. 1, which illustrates the known mass-5 energy levels, one sees that only $T = \frac{1}{2}$ states at 16.7 (16.65) and 20 MeV have been observed in ${}^5\text{He}$ (${}^5\text{Li}$) at high excitation. Nevertheless, since most of the reactions which have been used to search for states of ${}^5\text{He}$ or ${}^5\text{Li}$ were incapable of forming $T = \frac{3}{2}$ states, except through $T = \frac{1}{2}$ admixtures, it is perhaps not surprising that the analog states have not been observed.

It has been demonstrated that the (p,t) and $(p,{}^3\text{He})$ reactions readily populate analog states with $T = T(\text{target}) + 1$ in several light nuclei.⁷ An unsuccessful search for the mass-5 $T = \frac{3}{2}$ states utilizing these reactions on a ${}^7\text{Li}$ target has already been reported by this laboratory.⁸ As seen in Fig. 2, taken from Ref. 8, the spectra from the ${}^7\text{Li}(p,{}^3\text{He}){}^5\text{He}$ reaction revealed only the well-known 16.7- and 20-MeV states of ${}^5\text{He}$ in the region of high excitation, while the ${}^7\text{Li}(p,t){}^5\text{Li}$ spectra exhibited no peaks in this region other than from contaminants (see Ref. 8). The absence of transitions to the mirror states of ${}^5\text{Li}$ was attributed to the selection rule requiring $S = 0$ for the spin of the transferred neutron pair, which forbids formation of the 16.65-MeV [${}^4\text{S}_{3/2}$] and 20-MeV [${}^4\text{D}_{3/2,5/2}$] ${}^5\text{Li}$ states by

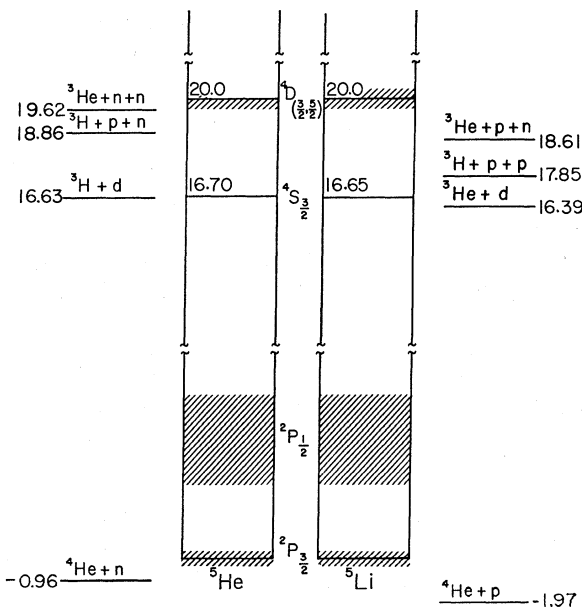


FIG. 1. Energy-level diagrams for ${}^5\text{He}$ and ${}^5\text{Li}$ including particle-decay thresholds, taken from Ref. 1.

[†] This work was done under the auspices of the U. S. Atomic Energy Commission.

* Present address: Physics Department, University of Southwestern Louisiana, Lafayette, Louisiana.

¹ T. Lauritsen and F. Ajzenberg-Selove, Nucl. Phys. 78, 1 (1966).

² A. I. Baž, V. I. Goldanskii, and Ya. B. Zeldovich, Usp. Fiz. Nauk. 85, 445 (1965) [English trans.: Soviet Phys.—Usp. 8, 177 (1965)].

³ R. C. Cohen, A. D. Kanaris, S. Margulies, and J. L. Rosen, Phys. Letters 14, 242 (1965).

⁴ F. C. Barker (The Australian National University, Canberra, Australia, private communication).

⁵ T. I. Kopaleishvili (Tbilisi State University, Tbilisi, U.S.S.R., private communication).

⁶ R. F. Fraser and B. M. Spicer, Australian J. Phys. 19, 893 (1966).

⁷ J. Cerny and R. H. Pehl, Phys. Rev. Letters 12, 619 (1964); J. Cerny, R. H. Pehl, and G. T. Garvey, *ibid.* 12, 234 (1964); C. Détraz, J. Cerny, and R. H. Pehl, *ibid.* 14, 708 (1965); J. Cerny, R. H. Pehl, G. Butler, D. G. Fleming, C. Maples, and C. Détraz, Phys. Letters 20, 35 (1966).

⁸ J. Cerny, C. Détraz, and R. H. Pehl, Phys. Rev. 152, 950 (1966).

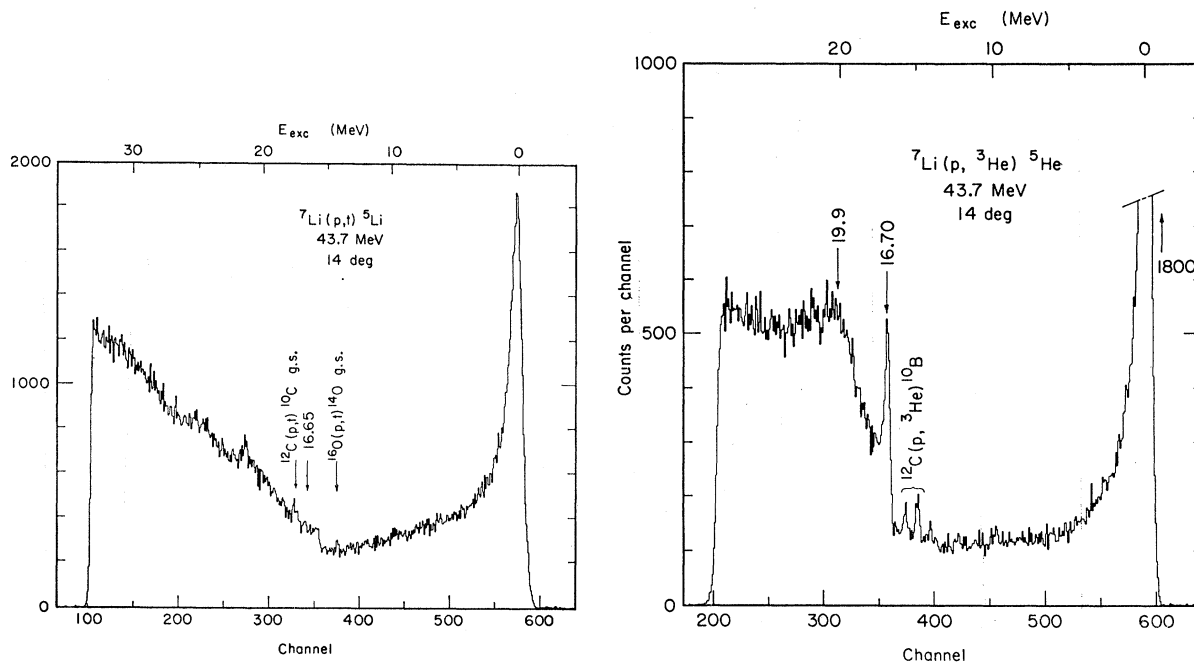


FIG. 2. The energy spectra of the ${}^7\text{Li}(p,t){}^5\text{Li}$ and ${}^7\text{Li}(p,{}^3\text{He}){}^5\text{He}$ reactions at 14° , taken from Ref. 8.

two-neutron pickup from the ${}^7\text{Li}$ ground state [${}^2P_{3/2}$]. Since the spin selection rule in the $(p,{}^3\text{He})$ reaction permits $S=0$ or 1 , the 16.7- and 20-MeV ${}^5\text{He}$ states are formed via the $S=1$ component. The absence of transitions corresponding to the known $T=\frac{1}{2}$ states of ${}^5\text{Li}$ in the excitation region of interest would seem to make this reaction a sensitive probe for the lowest $T=\frac{3}{2}$ state, which should be a doublet in intrinsic spin. Unfortunately, large continuum backgrounds might have obscured transitions with small cross sections and/or broad states.

We report in this paper on three further experiments on the properties of the mass-5 $T=\frac{3}{2}$ states. First, we have obtained triton spectra from the ${}^7\text{Li}(p,t){}^5\text{Li}$ reaction under conditions similar to those of the previous work, but with improved counting statistics. Second, data on coincidences between tritons, ${}^3\text{He}$'s, and α 's resulting from reactions of $p+{}^7\text{Li}$ have been collected in order to study the decay properties of intermediate ${}^5\text{He}$ and ${}^5\text{Li}$ states. Third, we have directly searched for ${}^5\text{H}$ states by observing ${}^8\text{B}$ energy spectra from the ${}^9\text{Be}(\alpha,{}^8\text{B}){}^5\text{H}$ reaction.

II. THE ${}^7\text{Li}(p,t){}^5\text{Li}$ REACTION

Figure 3 shows a triton spectrum at 14.1° obtained by bombarding an $800\ \mu\text{g}/\text{cm}^2$ self-supporting ${}^7\text{Li}$ target with 43.7-MeV protons from the Berkeley 88-in. cyclotron. Signals from a counter telescope consisting of $140\ \mu\text{m}$ ΔE , $3200\ \mu\text{m}$ E , and $600\ \mu\text{m}$ E -reject semiconductor detectors were fed to a Goulding-Landis⁹ particle

identifier. The summed $(\Delta E + E)$ pulses were then passed on to a 4096-channel analyzer gated so as to store 1024-channel energy spectra corresponding to selected portions of the identifier spectrum. An anti-coincidence requirement utilizing signals from the E -reject counter eliminated particles traversing the E counter. The complete spectrum was accumulated for $940\ \mu\text{C}$; the data in the inset were taken for $2200\ \mu\text{C}$ and summed over 4-channel intervals to improve the counting statistics. In obtaining these latter data, the beam intensity was increased and a relatively narrow window was set on the E amplifier output covering the excitation region of interest, thus maintaining a reasonable counting rate in the identifier.

Since the lowest mass-5 $T=\frac{3}{2}$ state configuration is probably $(1s)^3(1p)^2$, an $L=1$ angular-momentum transfer is required to form the ${}^5\text{Li}$ member. Angular distribution data in Ref. 8 indicated that 14° was a good angle for observing such an $L=1$ transition. The complete spectrum in Fig. 3 contains no obvious reasonably narrow peaks other than that of the ${}^5\text{Li}$ ground state. Positions of possible ${}^{12}\text{C}$ and ${}^{16}\text{O}$ contaminant peaks are indicated on the spectrum. The large continuum is primarily associated with the multiparticle final states listed at the top of the figure. This absence of peaks is an indication that the $T=\frac{3}{2}$ state(s) must lie at fairly high excitation and be broad: For example, assuming a hypothetical state at 20 MeV with a width of 500 keV, then an easily discernible peak would have appeared in the complete spectrum, provided the center-of-mass cross section was bigger than about $13\ \mu\text{b}/\text{sr}$. For comparison, (p,t) transitions to $T=\frac{3}{2}$ states under these experimental conditions possess peak cross sections

⁹ F. S. Goulding, D. A. Landis, J. Cerny, and R. H. Pehl, Nucl. Instr. Methods **31**, 1 (1964).

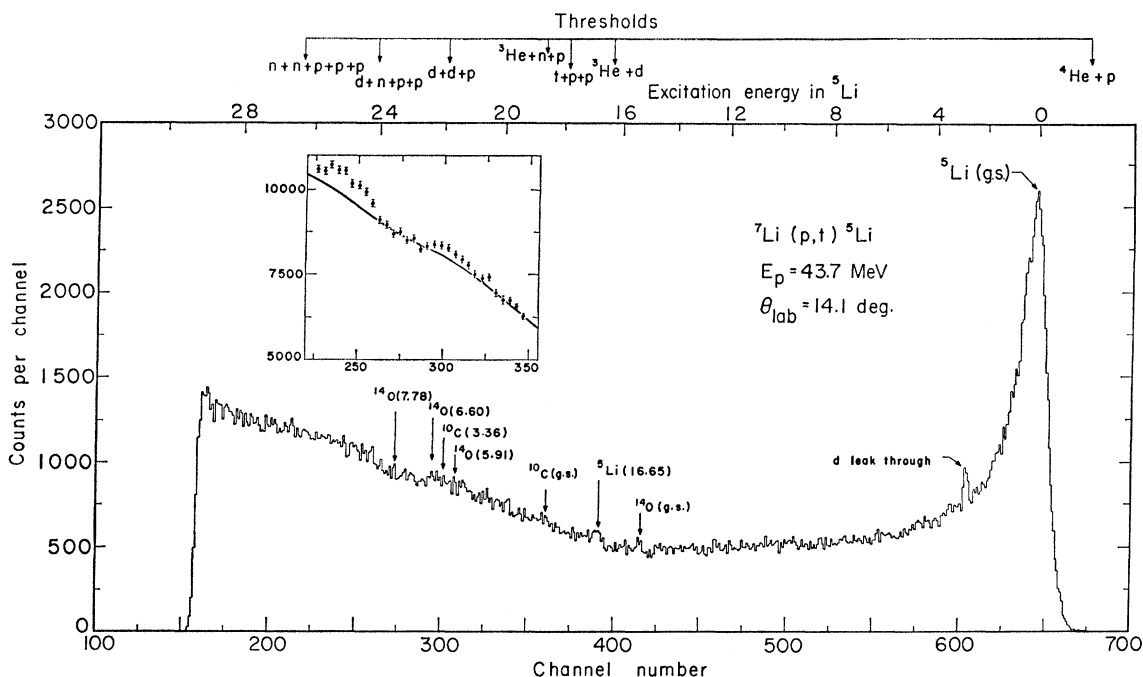


FIG. 3. The energy spectrum of the ${}^7\text{Li}(p,t){}^5\text{Li}$ reaction at 14.1° . The complete spectrum was accumulated for $940\ \mu\text{C}$, while the data in the inset were collected for $2200\ \mu\text{C}$. The positions of possible contaminant peaks are indicated as are the multiparticle breakup thresholds. The solid line in the inset is a composite phase-space distribution which is discussed in the text.

between about 50 and $140\ \mu\text{b}/\text{sr}$.¹⁰ In particular, the ${}^{19}\text{F}[\frac{1}{2}^+, T=\frac{1}{2}](p,t){}^{17}\text{F}[\frac{1}{2}^-, T=\frac{3}{2}]$ transition, which requires an $L=1$ pickup of a neutron pair, closely resembles a ${}^7\text{Li}[\frac{3}{2}^-, T=\frac{1}{2}](p,t){}^5\text{Li}[\frac{1}{2}^+, T=\frac{3}{2}]$ transition, which also requires an $L=1$ pickup of two neutrons. The calculated structure factors¹¹ appear comparable and the cross section of the ${}^{19}\text{F}$ transition is about $60\ \mu\text{b}/\text{sr}$ at 14° (lab).¹² If the analog state lies at higher excitation, then, of course, the sensitivity for observing the state decreases due to the rising continuum background and because the width of such a state is likely to increase.

Two broad peaks corresponding to 22 ± 0.5 and 25 ± 0.5 MeV excitation are apparent in the inset. The line in the figure represents a sum of the $t+\alpha+p$, $t+{}^3\text{He}+d$, and $t+d+d+p$ final-state phase-space distributions. This set of final states, along with their relative amplitudes, was chosen to minimize the residual area under the two peaks, subject to the requirement that the height of the resultant phase-space envelope did not exceed the height of the complete spectrum at any energy. The cross sections for the peaks with this phase-space background subtracted were 14 and $41\ \mu\text{b}/\text{sr}$, respectively; the width of both peaks corre-

sponded to approximately 1.5 MeV with respect to the ${}^5\text{Li}$ recoil system. It appears on the basis of the complete spectrum that ${}^{12}\text{C}$ contamination was negligible; however, from the known¹² ${}^{16}\text{O}(p,t){}^{14}\text{O}$ cross sections, it was estimated that at most 50% of the counts under the 22-MeV peak may have been due to the ${}^{14}\text{O}$ 6.60-MeV state. These cross sections should be considered as lower limits, provided that they can be associated with real ${}^5\text{Li}$ states; that is, we attribute no particular significance to the actual shape or magnitude of the phase-space distribution, so the actual cross sections may be larger than those given. It is well known that the observation of peaks at excitations higher than particle thresholds in the residual nucleus does not necessarily establish the existence of a corresponding state of this nucleus because the kinematics of possible multiparticle reactions are not fixed by a single-counter experiment. The resulting ambiguity in the interpretation of these peaks both with regard to their origin and their isospin was one of the reasons for performing the coincidence experiment, which is described below.

III. COINCIDENCE SPECTRA FROM THE $p+{}^7\text{Li}$ REACTION

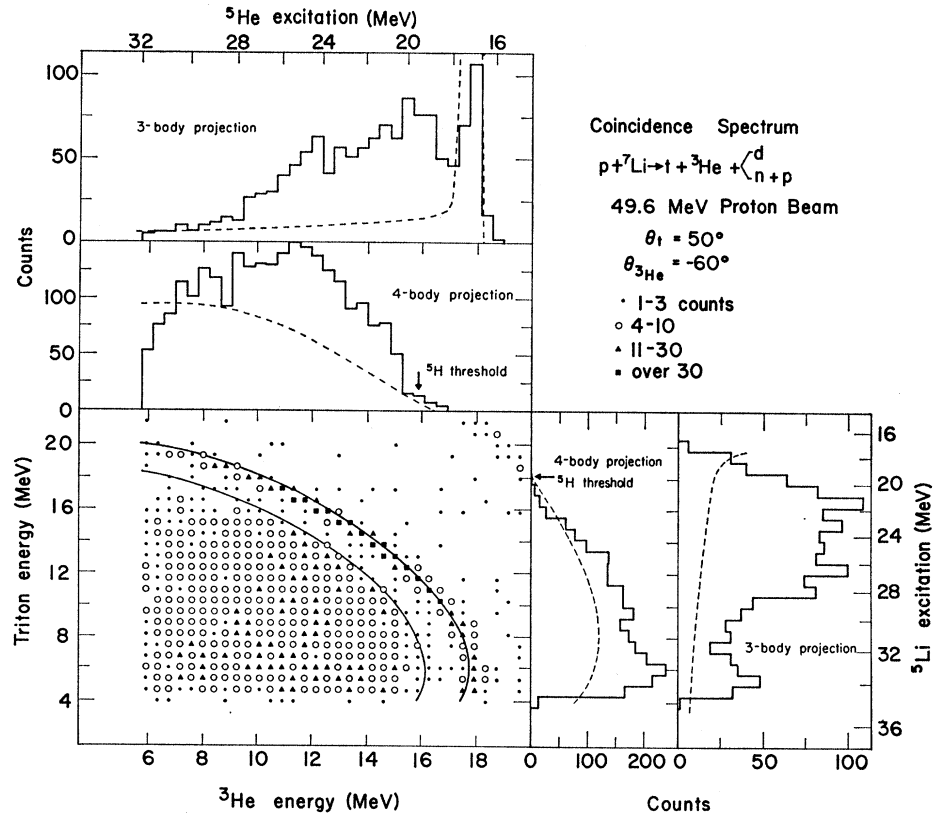
If the momenta of two particles of a three-particle final state are determined, then the kinematics of the reaction constrain all such events to lie along a curved line in the two-dimensional energy plane of the detected

¹⁰ C. Détraz, J. Cerny, and R. H. Pehl, Phys. Rev. Letters **14**, 708 (1965); J. Cerny, R. H. Pehl, G. Butler, D. G. Fleming, C. Maples, and C. Détraz, Phys. Letters **20**, 35 (1966); J. C. Hardy and D. J. Skyrme, *Isobaric Spin in Nuclear Physics*, edited by J. D. Fox and D. Robson (Academic Press Inc., New York, 1966), p. 701.

¹¹ N. K. Glendenning, Phys. Rev. **137**, B102 (1965).

¹² D. G. Fleming and J. Cerny (unpublished).

FIG. 4. A triton (50°), ${}^3\text{He}$ (-60°) coincidence spectrum. The solid lines in the two-dimensional array are the three- and four-particle final-state kinematic curves. Projections of the data onto both energy axes are shown; the phase-space distributions are given by the dashed lines for comparison. If ${}^5\text{H}$ is bound, the excitation of the lowest $T = \frac{3}{2}$ state of either ${}^5\text{He}$ or ${}^5\text{Li}$ is less than ~ 19.5 MeV, which is indicated by the arrow in the four-particle spectra.



particles.¹³ Sequential reactions proceeding through well-defined two-particle intermediate states will be characterized by peaks lying along the curve. The kinematical behavior of these peaks, as the detector angles are varied, often provides sufficient information to decide unambiguously which two-particle states are involved.

Triton-triton, triton- ${}^3\text{He}$, triton- α , ${}^3\text{He}$ - ${}^3\text{He}$, and ${}^3\text{He}$ - α coincidences from reactions of $p + {}^7\text{Li}$ yield information concerning the three- and four-particle final states listed in Table I. Various sequential reactions leading to three-particle final states are given explicitly in the table; the much larger set of possible sequential reactions yielding four-particle final states is not shown. The three-particle reactions 1, 2, 4, and 7 are interesting with respect to intermediate mass-5 states which decay by breakup into two particles. Similar four-particle sequential reactions also provide information on intermediate mass-5 states which breakup into three particles; however, the momenta of all four particles are not determined by double coincidence data so that four-particle events are confined to a region of the energy plane bounded by a curve given by kinematics. With coincidence data substantial improvement over the single detector system triton results was anticipated: (1) The "signal-to-noise" ratio of peaks relative to the

continuum should be enhanced with coincidence data since the laboratory cone angle of decay particles from ${}^5\text{He}$ or ${}^5\text{Li}$ states is usually smaller than 4π . (2) The decay properties of intermediate states, i.e., whether the state decays into two or three particles, are uniquely determined by the kinematics. The latter effect is particularly relevant to the search for the mass-5 $T = \frac{3}{2}$ states. Reference to Fig. 1 shows that in order to satisfy the isospin selection rules, pure $T = \frac{3}{2}$ states must decay by emission of three particles,¹⁴ whereas $T = \frac{1}{2}$ states may decay by emission of either two or three particles (for the latter states penetrability and phase-space

TABLE I. Multiparticle reactions of $p + {}^7\text{Li}$.

| 3-particle final state | 4-particle final state |
|--|---|
| $t + {}^5\text{Li}^* \rightarrow t + {}^3\text{He} + d$ (1) | } $t + {}^3\text{He} + n + p$ |
| ${}^3\text{He} + {}^5\text{He}^* \rightarrow {}^3\text{He} + t + d$ (2) | |
| $d + {}^5\text{Li}^* \rightarrow d + t + {}^3\text{He}$ (3) | |
| $t + {}^5\text{Li}^* \rightarrow t + \alpha + p$ (4) | } $t + {}^3\text{He} + n + p$ $t + t + p + p$ ${}^3\text{He} + {}^3\text{He} + n + n$ |
| $\alpha + {}^4\text{He}^* \rightarrow \alpha + t + p$ (5) | |
| $p + {}^7\text{Li}^* \rightarrow p + t + \alpha$ (6) | |
| ${}^3\text{He} + {}^5\text{He}^* \rightarrow {}^3\text{He} + \alpha + n$ (7) | |
| $\alpha + {}^4\text{He}^* \rightarrow \alpha + {}^3\text{He} + n$ (8) | |
| $n + {}^7\text{Be}^* \rightarrow n + {}^3\text{He} + \alpha$ (9) | |

¹⁴ Possible sequential decay of $T = \frac{3}{2}$ states involving mass-4 $T = 1$ states + nucleon effectively yield three particles, since the lowest $T = 1$ states are themselves particle unstable. [See, for example, J. Cerny, C. Détraz, and R. H. Pehl, Phys. Rev. Letters 15, 300 (1965)].

¹³ Č. Zupančič, Nuclearni Inštitut Jožef Stefan Report No. R-429, 1964 (unpublished).

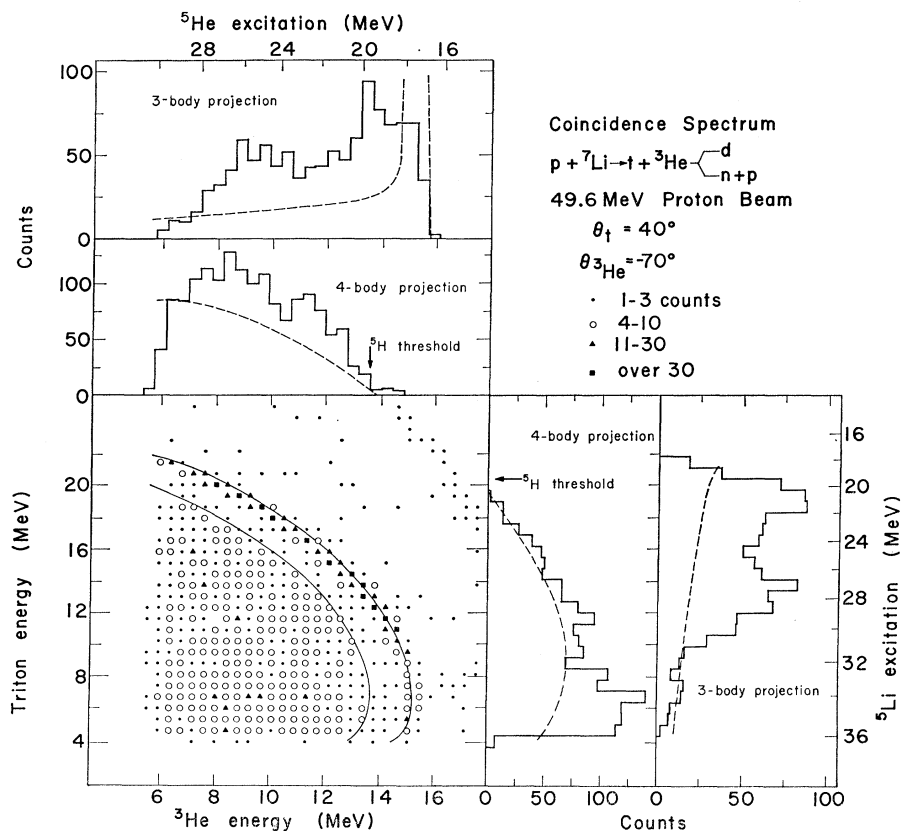


FIG. 5. A triton (40°), ${}^3\text{He}(-70^\circ)$ coincidence spectrum. See caption of Fig. 4.

volume effects probably favor two-particle decay near the three-particle thresholds). For example, events from reaction (2) in Table I proceeding through the 20-MeV [${}^4D_{3/2,5/2}$] ${}^5\text{He}$ intermediate state are expected to appear on a narrow segment along the three-particle curve in the triton- ${}^3\text{He}$ coincidence array. On the other hand, a sharp ${}^5\text{He}$ $T=3/2$ state at 20 MeV decaying to $t+n+p$ would manifest itself by events falling along a straight line perpendicular to the ${}^3\text{He}$ energy axis and lying in the four-particle region of the array. The kinematic limit of this region is separated by the 2.3-MeV deuteron binding energy from the three-particle curve. The distribution of events along this line with respect to triton energy depends on the dynamics of the decay; e.g., if the n - p final-state interaction were dominant, then the line would degenerate to a point near the four-particle kinematic limit corresponding to the pseudo three-particle final state ${}^3\text{He}+t+d^*$. In any case a projection of these events onto the ${}^3\text{He}$ energy axis would yield a peak corresponding to the ${}^5\text{He}$ 20-MeV excitation energy.

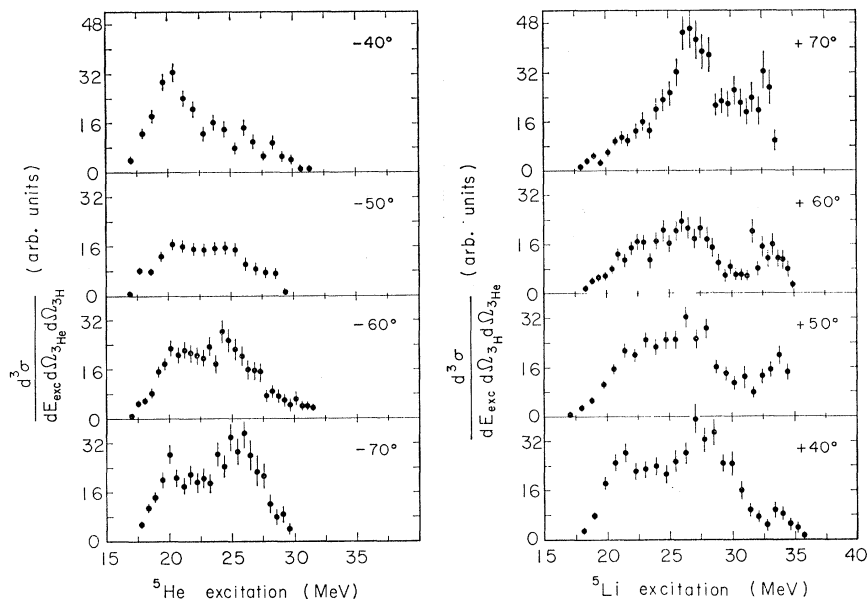
The coincidence experiments were performed with a 49.6-MeV proton beam focused to 60×100 mils on a $500\text{-}\mu\text{g}/\text{cm}^2$ ${}^7\text{Li}$ self-supporting target. One counter telescope (system 1), consisting of $81\text{-}\mu$ ΔE , $3050\text{-}\mu$ E , and $510\text{-}\mu$ E -reject semiconductor detectors, subtended 0.6 msr; the second telescope (system 2) consisting of $32\text{-}\mu$ ΔE and $1000\text{-}\mu$ E detectors subtended 3.84 msr.

Pulses from system 1 were fed to a particle identifier plus router system adjusted to provide signals corresponding to triton or ${}^3\text{He}$ particles. Pulses from system 2 were fed to a second particle identifier plus router system adjusted to pass triton, ${}^3\text{He}$, or α routing signals if the E pulse was in fast coincidence ($2\tau=50$ nsec) with the ΔE pulse from system 1. If an additional slow coincidence requirement on the routing signals from the two systems was satisfied, then the two $(\Delta E+E)$ total energy pulses from the telescopes and the appropriate two routing signals from both identifier-router systems were fed to an eight-channel analog buffer unit coupled to a 4096-channel analog-to-digital converter.¹⁵ The digital numbers were read by an on-line PDP-5 computer which stored the events on magnetic tape; in addition, six 32×32 two-dimensional energy arrays were stored in core to enable data monitoring on an oscilloscope display during the experiment.

Typical coincidence arrays are shown in Figs. 4 (and 5), in which tritons were counted at 50° (40°) and ${}^3\text{He}$'s at -60° (-70°). The rather large acceptance angles, necessitated by the expected small cross sections, meant the over-all energy resolutions of systems 1 and 2 were only about 0.5 and 1.0 MeV, respectively. Since relatively few events were collected, the data on mag-

¹⁵ F. S. Goulding, L. B. Robinson, and F. Gin (to be published); University of California Radiation Laboratory Report No. UCRL-16580, p. 224, 1966 (unpublished).

FIG. 6. Projections of the triton- ${}^3\text{He}$ three-particle final-state coincidence data taken at $(40^\circ, -70^\circ)$ and $(50^\circ, -60^\circ)$. The spectra on the left are obtained by projection onto the ${}^3\text{He}$ energy axis, and transformation to the ${}^5\text{He}$ recoil system; similarly, the spectra on the right are obtained by projection onto the triton axis and transformation to the ${}^5\text{Li}$ recoil system.



netic tape were sorted and condensed to 64×64 channel arrays. The three- and four-particle final states are cleanly separated in the figure. The kinematic curves for these final states are shown in the arrays. A few events resulting from α -particle leak-through into the ${}^3\text{He}$ region of the particle identifier spectrum appear in the upper right corner of the arrays, but the relatively small negative Q value of the $t + \alpha + p$ reaction makes the effect negligible. Projections of both the three- and four-particle events, proportional to $d^3\sigma/dE_3^l d\Omega_3^l d\Omega_4^l$, onto each energy axis are given in the figures. The numbers denote particles 3 and 4 in the symbolic reactions $[1+2 \rightarrow 3+4+5]$ or $[1+2 \rightarrow 3+4+5+6]$, and l refers to laboratory coordinates. Excitations of the $(4+5)$ or $(4+5+6)$ recoil systems are also indicated along with E_3^l in the figures. The phase-space volume in both figures is given by the dotted lines for comparison with the data. The triton phase-space distributions are normalized with respect to the ${}^3\text{He}$ distributions which in turn are normalized to the data at 8 MeV ${}^3\text{He}$ energy. The phase space is singular along the ${}^3\text{He}$ axis where the three-particle kinematic curve is perpendicular to this axis. However, the peak obtained by projecting this segment of the curve in either figure onto the triton axis implies that phase space is not solely responsible for the observed peak in the ${}^3\text{He}$ spectrum. These projections are discussed in more detail below.

Further coincidence arrays will not be shown¹⁶; qualitatively the remaining triton- ${}^3\text{He}$ data are similar

¹⁶ The triton- α data are dominated by a broad peak corresponding to either a 29-MeV ${}^7\text{Li}$ ($\Gamma \sim 4$ MeV), a 32-MeV ${}^4\text{He}$ ($\Gamma \sim 6$ MeV), or a 20-MeV ${}^5\text{Li}$ ($\Gamma \sim 10$ MeV) state; the last possibility can be rejected on the basis of known level data. The ${}^3\text{He}$ - α arrays also exhibit a broad peak corresponding to either a 29-MeV ${}^7\text{Be}$ ($\Gamma \sim 3$ MeV), a 34-MeV ${}^4\text{He}$ ($\Gamma \sim 8$ MeV), or a 15.5-MeV ${}^5\text{He}$ ($\Gamma \sim 10$ MeV) state. Again, the last possibility can be ruled

to those shown in Figs. 4 and 5. Data were collected at two pairs of angles, $(50^\circ, -60^\circ)$ and $(40^\circ, -70^\circ)$, so that triton- ${}^3\text{He}$ projections at four angles were obtained. These are shown in Fig. 6 where the three-particle spectra have been transformed from the laboratory coordinate system (finite geometry effects have not been included) to one at rest with respect to the recoil ${}^5\text{He}$ or ${}^5\text{Li}$ nuclei to facilitate comparison of the spectra at different angles. Peaks on the right side of the figure obviously are related to peaks on the left side since the spectra were obtained from the same three-particle curve in the original two-dimensional energy plane. A trivial exception occurs where the ${}^5\text{He}$ counterpart to the peak at 34 MeV in ${}^5\text{Li}$ disappears because, due to the tangent effect pointed out in the discussion of Fig. 4, the ${}^5\text{He}$ Jacobian vanishes at this point.

It is clear from Fig. 6 that the width of the observed peaks, together with the poor counting statistics, precludes their unambiguous association with states in one of the various two-particle systems on the basis of kinematic shifts alone. [In fact, the two pairs of angles were chosen to maximize the laboratory energy of the decay particles from intermediate mass-5 states at around 22 MeV, so that kinematic shifts were typically on the order of only several hundreds of keV.] However, the peak at 20 MeV in ${}^5\text{He}$ (and the associated peak at an *apparent* excitation of 27 MeV in ${}^5\text{Li}$) is consistent with Ref. 8, where the 20 MeV ${}^5\text{He}$ state was found to have a relatively large cross section (at 40° the center-of-mass cross section was $60 \mu\text{b}/\text{sr}$) and a width of

out. The existence of ${}^4\text{He}$ states at about 30 MeV is known (see Ref. 17); unfortunately, little information is available on mass-7 states at the appropriate excitations. Since these data are inconclusive and are not relevant to the mass-5 states, they are ignored in the remaining discussion.

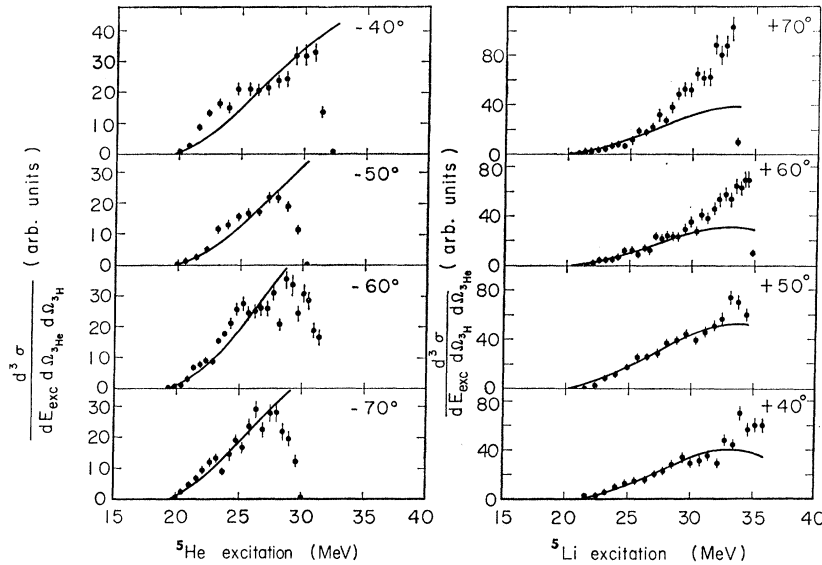


FIG. 7. Projections of the triton- ^3He four-particle final-state coincidence data. The spectra on the left are obtained by transformation of the coincidence data into the ^5He recoil system and projection onto the ^3He axis and those on the right by transformation of the data into the ^5Li recoil system and projection onto the triton axis as described in the text. The solid lines are phase-space fits to the spectra.

approximately 2.7 MeV. A width of 3 ± 0.6 MeV is obtained from the -40° ^5He spectrum in these data. Figure 6 also presents peaks corresponding to a state at 21.5 MeV in ^5Li or at 25 MeV in ^5He , or perhaps to contributions from both such states. Any of these possibilities is consistent with the triton spectrum discussed previously, where "peaks" tentatively associated with 22- and 25-MeV ^5Li states were found, provided mirror states of ^5He are also postulated. Unfortunately we are unable to make any additional conclusion from the present data except that it appears any new states at 22 or 25 MeV would more likely have $T = \frac{1}{2}$. In fact, from these coincidence data alone, it is conceivable that an intermediate ^6Li state at about 34.6 MeV with $\Gamma \lesssim 0.7$ MeV could account for both pairs of peaks discussed above. We regard this as unlikely both because the width seems narrow for such a highly excited state, and because the interpretation of both pairs of peaks as due to mass-5 states is consistent with the single-counter results discussed above and with Ref. 8.

The peak at about 34 MeV in the ^5Li spectra near the experimental cutoff is probably due to the mirror of the $(1s)^{-2}$ ^6He state previously observed in the $^7\text{Li}(\pi^+, 2p)^{-5}\text{He}$ reaction,¹⁷ although once again we cannot rule out an intermediate ^6Li state at about 30.8 MeV on the basis of our data alone.

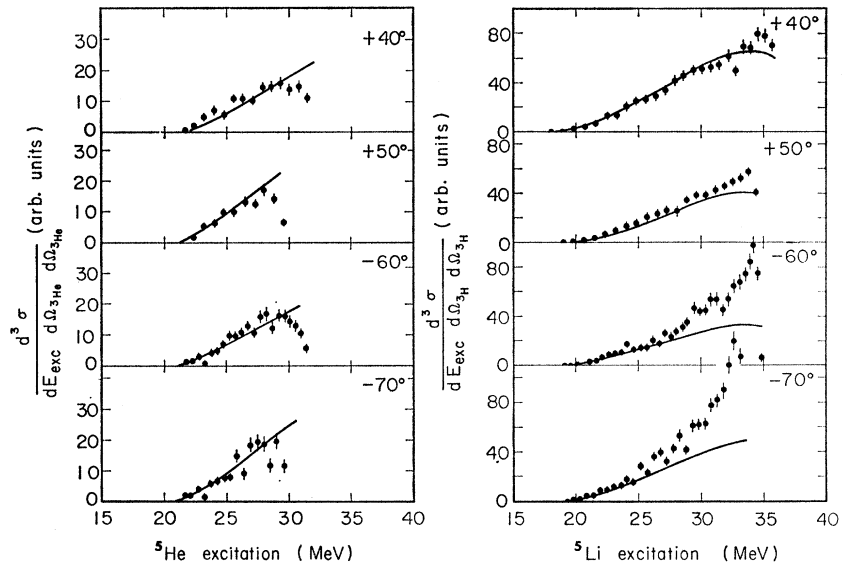
As has already been stressed, a primary reason for performing the coincidence experiment was that $T = \frac{3}{2}$ intermediate mass-5 states should decay into three particles if such decay is energetically allowed, so that these events lead to four-particle final states. Projections of all the four-particle data are shown in Figs. 7 and 8. Figure 7, containing the triton- ^3He data, is the analog to Fig. 6, where the three-particle spectra are shown. As in Fig. 6, the four-particle spectra have been trans-

formed to the recoil ^5He or ^5Li coordinate systems. The four-particle two-dimensional energy spectra in Figs. 4 and 5, which are proportional to $d^4\sigma/dE_3'dE_4'd\Omega_3'd\Omega_4'$, are first transformed to the appropriate recoil system and then integrated over particle-4 energy (the notation is the same as defined earlier). The relative heights of the resulting spectra given in the figures should not be directly compared, since the particle-4 integration interval depends both on the low energy cutoff of the particle-4 counter (which is different for the two counter-telescopes), and on the kinematics associated with the counter angles. In contrast to Figs. 6 and 7, where two spectra in the same row are obtained from the same two-dimensional energy spectrum, the spectra on the left side of Fig. 8 are obtained from the ^3He - ^3He coincidence data while the spectra on the right side are derived from the triton-triton data. Hence, the first and fourth spectrum in each column represent the two projections of the $(40^\circ, -70^\circ)$ data while the 2nd and 3rd spectrum in each column are obtained from the $(50^\circ, -60^\circ)$ data.

In general, the four-particle spectra in both figures simply rise with increasing excitation energy and possess no well-defined peak structure which might be associated with the sought analog states. The ^5He spectra in Fig. 7 are exceptions, exhibiting a broad peak extending from about 22 to 25 MeV, but there is no hint of this structure in the ^5Li spectra in the same figure. This asymmetry still persists (although it is less pronounced) when the ^5He projected spectra are obtained by integrating over those triton energies corresponding to the ^3He energies which have been integrated to give the ^5Li spectra on the right side of Fig. 7; therefore, the bump in the ^5He spectra is not solely due to integrating over the many low-energy triton events which are apparent in the ^5Li projections. This bump is not understood and one might consider it to arise from the

¹⁷ G. Charpak, G. Gregoire, L. Massonnet, J. Saudinos, J. Favier, M. Gusakov, and M. Jean, Phys. Letters 16, 54 (1965).

FIG. 8. Projections of the ${}^3\text{He}$ - ${}^3\text{He}$ four-particle final-state coincidence data are shown on the left and projections of the triton-triton four-particle final-state data are shown on the right after transformation to the ${}^5\text{He}$ and ${}^5\text{Li}$ recoil systems, respectively. The solid lines are phase-space fits to the spectra.



same states at 22 and/or 25 MeV as were earlier observed in the three-particle data; however, we do not feel that we can associate it or the ${}^5\text{Li}$ states at these energies with the desired $T = \frac{3}{2}$ states *since comparable structure is not observed in any of the ${}^5\text{Li}$ four-particle spectra*. It has been demonstrated⁷ several times that the ratio of (p,t) to $(p,{}^3\text{He})$ cross sections to analog states is primarily dependent only on isospin-coupling coefficients and phase-space factors which for the present case give a ratio of unity.

Calculated four-particle phase-space distributions have been fitted by eye to the spectra in Figs. 7 and 8 for comparison. Except for the bump in the ${}^5\text{He}$ spectra mentioned above, the fits approximate rather well the shapes of the spectra extending from the experimental cutoffs up to about 27-MeV excitation energy in both ${}^5\text{He}$ and ${}^5\text{Li}$. Unfortunately, the data do not extend down to the three-particle decay thresholds given in Fig. 1, so that decays from hypothetical states below about 20 MeV in ${}^5\text{He}$ and about 20.5 MeV in ${}^5\text{Li}$ could not have been detected in the triton- ${}^3\text{He}$ data. The ${}^3\text{He}$ - ${}^3\text{He}$ data in Fig. 8 cut off at about 21.5 MeV in ${}^5\text{He}$, whereas the triton-triton data extend down to about 19.0 MeV in ${}^5\text{Li}$. Therefore these triton-triton data permit examination for three-particle decay of states lying at lower excitation in mass-5 than any of the other data. We could not have observed a ${}^5\text{Li}$ state with an open $T = \frac{3}{2}$ decay mode lying between the $t+p+p$ threshold at 17.85 MeV and 19 MeV; however, such a state would probably be narrow enough to be discernible in the triton singles data discussed above.

Since we find no indication of mass-5 $T = \frac{3}{2}$ states in the four-particle data, it is of interest to estimate singles cross-section upper limits for formation of such states. The arbitrary units corresponding to the $+40^\circ$ ${}^5\text{Li}$ spectrum in Fig. 8 are equivalent to $0.10 \pm 0.03 \mu\text{b}/\text{MeV sr}^2$, so that the absolute cross section at 20

MeV ${}^5\text{Li}$ excitation is $0.28 \pm 0.09 \mu\text{b}/\text{MeV sr}^2$. To obtain the singles cross section, it is assumed a $T = \frac{3}{2}$ state at this excitation could decay into $t+p+p$ with no dependence either on the angle of emission or on the energy of the decay triton with respect to the ${}^5\text{Li}$ rest system. The former assumption will be valid, provided the hypothetical state has a spin of $\frac{1}{2}$ as expected for the lowest $T = \frac{3}{2}$ state; the latter assumption is necessitated by the experimental cutoff which permits observation of roughly 75% of the total triton decay energy spectrum allowed by kinematics. Correcting for the unobserved portion of the decay energy spectrum, multiplying by 4π , and dividing by the square of the Clebsch-Gordan isospin coupling coefficient for the $t+p+p$ component of a $T = \frac{3}{2}$ state, then the absolute singles cross section related to the coincidence data is estimated to be $14.3 \pm 4.8 \mu\text{b}/\text{MeV sr}$. Therefore, if such a $T = \frac{3}{2}$ state exists at 20-MeV excitation with a width less than 1 MeV, it should be apparent in the data if the ${}^7\text{Li}(p,t){}^5\text{Li}$ cross section is larger than about $5 \mu\text{b}/\text{sr}$ at this angle.

To conclude this section, no evidence is found for ${}^5\text{He}$ or ${}^5\text{Li}$ states which decay via $T = \frac{3}{2}$ modes, implying that the analog states are very broad. It is, of course, possible that these states could have sufficiently mixed isospin that decay by $T = \frac{1}{2}$ modes is favored.

IV. THE ${}^9\text{Be}(\alpha,{}^8\text{B}){}^5\text{H}$ REACTION

Observation of ${}^8\text{B}$ ions from reactions of α particles on ${}^9\text{Be}$ targets permits direct examination of the ${}^5\text{H}$ system. An 129-MeV α -particle beam was used to bombard a self-supporting $650 \mu\text{g}/\text{cm}^2$ ${}^9\text{Be}$ target and, in addition, a $250 \mu\text{g}/\text{cm}^2$ ${}^{12}\text{C}$ target for calibration purposes. Two four-counter telescopes were used: one positioned both at 10° and 14.1° consisted of a $61\text{-}\mu$ $\Delta E2$ counter, a $32\text{-}\mu$ $\Delta E1$ counter, a $300\text{-}\mu$ E counter,

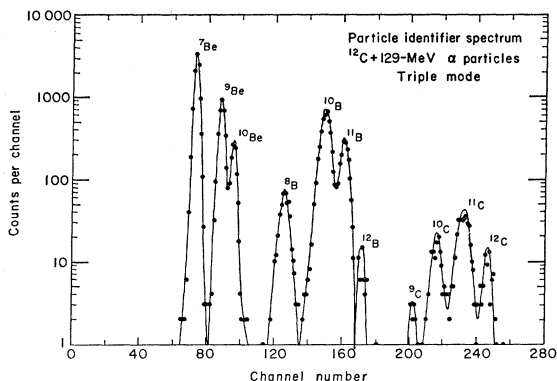


FIG. 9. Triple-counter particle-identifier spectrum resulting from the 129-MeV α -particle bombardment of ^{12}C , showing the separation of Be, B, and C isotopes; taken from Ref. 19.

and a 500- μ E -reject counter; the other, at 11.2° , consisted of a 37- μ $\Delta E2$ counter, a 23- μ $\Delta E1$ counter, a 300- μ E counter, and a 500- μ E -reject counter. Signals from these detectors were fed to two triple-counter particle identifiers which have been previously described.¹⁸ An identifier spectrum collected at 10° is shown in Fig. 9. ^8B energy spectra were collected by gating a pulse-height analyzer with appropriate routing signals from the identifiers. These data were obtained while establishing the feasibility of using these identifiers for particles of $Z=4, 5$, and 6, and a description of the general experimental setup has been published elsewhere.¹⁹

A $^{12}\text{C}(\alpha, ^8\text{B})^8\text{Li}$ energy spectrum is shown in Fig. 10, where the data from both telescopes have been added together after the necessary kinematic adjustments. The energy resolutions of both systems were comparable, being about 440-keV FWHM for the ^8Li ground-state peak. Most of the known¹ states of ^8Li are apparent in the spectrum; however, the states lying above the 2.26-MeV state are quite broad and are not resolved (in this part of the spectrum the data have been summed over four channels and divided by four in order to improve the counting statistics). The shape of the continuum, beginning at the $^7\text{Li}+n$ threshold, is fit by the three-particle phase-space distribution shown in the figure. The average center-of-mass cross sections at the three angles are 0.54 $\mu\text{b}/\text{sr}$ and 0.88 $\mu\text{b}/\text{sr}$ for the ^8Li ground state and 2.26-MeV state, respectively.

Figure 11 presents the ^8B spectra from the $\alpha+^9\text{Be}$ reaction. The energy calibration was taken from the ^8Li data discussed above. No sharp states are evident in the data from either telescope. Instead, the spectra rise rather smoothly above the threshold for ^5H particle stability (relative to decay into $t+n+n$). We have

¹⁸ F. S. Goulding, D. A. Landis, J. Cerny, and R. H. Pehl, IEEE Trans. Nucl. Sci. 13, 514 (1966).

¹⁹ J. Cerny, S. W. Cosper, G. W. Butler, H. Brunnader, R. L. McGrath, and F. S. Goulding, Nucl. Instr. Methods 45, 337 (1966).

attempted to fit the spectra with arbitrary combinations of three- and four-particle phase-space distributions but with little success. Both spectra exhibit a residual "peak" extending from near the threshold to about 20-MeV excitation in ^5H peaking in both cases at 11.6-MeV excitation above threshold. This peak can certainly not be associated with a single state of ^5H . Whether it results from several broad states and/or angular momentum or other effects not considered in the phase-space calculations is not clear. It is possible to set an upper limit on the cross section of a well-defined state of ^5H . If the state is narrower than about 1 MeV and lies lower than 1.5 MeV above the threshold, it would have been obvious in the data if it possessed an average cross section at the two angles larger than 22 nb/sr or, in other words, larger than 1/25 the cross section for the $^{12}\text{C}(\alpha, ^8\text{B})^8\text{Li}$ g.s. reaction. If ^5H is just bound, then it would be apparent in the data if the average cross section were about 1/88 that of ^8Li g.s. reaction.

V. CONCLUSIONS

The triton spectra first discussed contained very small broad peaks corresponding to possible 22- and 25-MeV states of ^5Li . The three-particle coincidence data are consistent with the existence of mass-5 states at these energies but are not unambiguous, making the evidence for these states tentative. On the other hand, we find no evidence for mass-5 states having the expected $T=\frac{3}{2}$ decay properties. In the vicinity of 20-MeV excitation in ^5Li (the region of interest with respect to the particle stability of ^5H) cross section upper limits for well-defined $T=\frac{3}{2}$ states have been estimated which are substantially smaller than (p,t) , $(p,^3\text{He})$ cross sections for formation of $T=\frac{3}{2}$ states in other nuclei. Further, the $^9\text{Be}(\alpha, ^8\text{B})^8\text{H}$ data exhibit no peaks which can be associated with sharp ^5H states. Therefore, we conclude from these data that the lowest mass-5 $T=\frac{3}{2}$ states exist at relatively high excitation above the

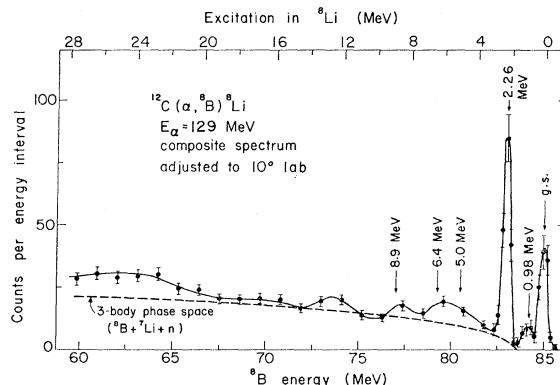


FIG. 10. A composite $^{12}\text{C}(\alpha, ^8\text{B})^8\text{Li}$ energy spectrum of data taken at 10° , 11.2° , and 14.1° (lab). The dashed line is a phase-space fit to the $^8\text{B}+^7\text{Li}+n$ continuum and the positions of most previously established ^8Li levels are marked.

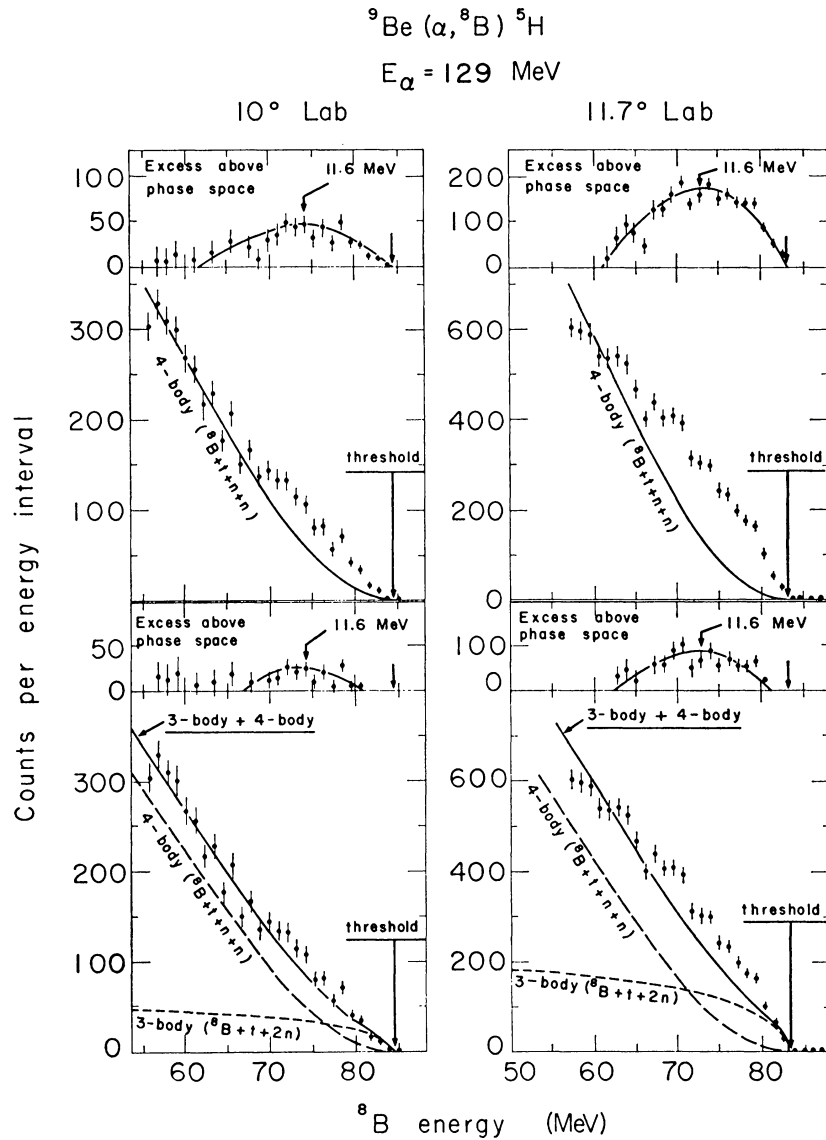


FIG. 11. The ${}^9\text{Be}(\alpha, {}^8\text{B}) {}^5\text{H}$ energy spectra at 10° and 11.7° (lab). The spectra are fitted with four-particle (${}^8\text{B}+t+n+n$) phase-space distributions in the upper half of the figure and with a sum (solid line) of three-particle (${}^8\text{B}+t+2n$) and four-particle (${}^8\text{B}+t+n+n$) phase-space distributions (dashed lines) in the lower half of the figure. In both cases, the spectra exhibit an "excess" above the phase-space curves which peak at ~ 11.6 MeV excitation above the $t+n+n$ threshold, but contain no evidence for well-defined states of ${}^6\text{H}$.

relevant three-particle decay thresholds and, hence, are quite broad. These results are qualitatively consistent with the theoretical predictions⁴⁻⁶ that ${}^6\text{H}$ is unbound by at least several MeV.

ACKNOWLEDGMENT

We wish to thank George Goth for his assistance in various phases of these experiments and their analysis.